

Heat Mitigation in Cities: A Catalyst for Building Energy Saving

Mat Santamouris (✉ m.santamouris@unsw.edu.au)

UNSW

Article

Keywords: Building energy use, Urban building energy modelling, Building performance simulation, Mitigation and adaptation strategies, Advanced heat mitigation technologies

Posted Date: September 19th, 2023

DOI: <https://doi.org/10.21203/rs.3.rs-3344548/v1>

License:  This work is licensed under a Creative Commons Attribution 4.0 International License. [Read Full License](#)

Additional Declarations: There is **NO** Competing Interest.

Version of Record: A version of this preprint was published at Nature Cities on January 11th, 2024. See the published version at <https://doi.org/10.1038/s44284-023-00005-5>.

Abstract

Overheating of cities increases the cooling energy consumption of buildings and the corresponding peak electricity demand. Advanced urban heat mitigation technologies that involve the use of super cool photonic materials combined with properly designed green infrastructure, lower the urban ambient and land surface temperatures and reduce the cooling energy consumption at the city scale. Here, we present and report the results of the world's largest heat mitigation project in Riyadh, KSA. Daytime radiative coolers as well as cool and super cool materials combined with irrigated or non-irrigated greenery, have been used to design eight holistic and integrated heat mitigation scenarios, properly assessed by mesoscale climatic models covering the whole city. We assessed the impact of the scenarios as well as the corresponding energy benefits of 3323 urban buildings. An impressive decrease of the peak ambient temperature, up to 4.5°C, is calculated, consisting of the highest reported urban cooling performance, while the cooling degree hours in the city decrease by up to 26%. We found that innovative urban heat mitigation strategies contribute to remarkable cooling energy conservation by up to 16%, while the combined implementation of heat mitigation and energy adaptation technologies result in a decrease in the cooling demand by up to 35%. It is the first article investigating and reporting the large-scale energy benefits of modern heat mitigation technologies implemented in large cities as well as the dynamic and complex interdependencies between urban buildings and the urban environment as well as the suitability and the corresponding cooling and energy conservation potential of current and advanced heat mitigation technologies. It finally explores pathways to optimise urban heat mitigation and the related energy conservation strategies in cities.

1. Introduction

Cities are one of the largest energy consuming groups and emitters of greenhouse gases in the world. Urban areas offer a large potential for improvement of energy efficiency and reduction of greenhouse gases. Cities exhibit higher temperatures than the surrounding suburban and rural areas because of their positive thermal balance [1]. Global climate change is synergistically affecting the temperature of cities, increasing the magnitude of overheating [2]. More than 13000 cities are exhibiting overheating problems up to 10.0°C, while more than 1.7 billion people live under severe overheating conditions [3, 4].

Urban overheating has a serious impact on human life [5]. It increases both the cooling energy consumption of buildings and the peak electricity demand of buildings obliging utilities to build additional power plants for supply security, decreases human productivity, increases the concentration of harmful air pollutants and especially of the ground level ozone, and surges heat-related mortality and morbidity while it intensifies human aggressivity and the related mental health problems [5].

Assessment of the cooling penalty induced by urban overheating involving data from 18 world cities has shown that the cooling energy demand of reference buildings has increased by 23% between 1970 and 2010, while the corresponding average energy penalty at the city scale caused by the increased urban temperatures is approximately $0.73 \pm (0.64)$ kWh/m²/°C, the average annual global energy penalty per person is $230 \pm (120)$ kWh/p, and the average annual global energy penalty per person and degree of temperature increase is $78 \pm (47)$ kWh/p/°C [6].

Increased urban temperatures result in a substantial surge in the peak electricity demand during the summer period. Data from 11 urban studies revealed that the average power penalty and the corresponding additional electricity demand induced by urban overheating is close to 21 Watts (± 10.4) per degree of temperature increase and per person [7].

Overheating affects the generation capacity of the power plants and increases the total number of major electrical grid failure events. An increase of 1°C in the ambient temperature decreases the output of thermal and nuclear power plants by 0.6% and 0.8%, respectively [8]. According to (9), the major electrical failure events in the USA have increased from 45 to 125 in the period 2015–2020.

Extreme ambient temperatures affect the price of electricity. During the 2022 heat wave in France, increased river temperatures seriously reduced the operational capacity of the nuclear power plants and resulted in day-ahead baseload power prices about 10 times higher than the prices between 2017 and 2021 [9].

Forecasts about the future climatic conditions in cities under various emission scenarios have shown that the minimum and maximum temperatures may increase substantially [10]. Depending on the local climatic characteristics, the forecasted increase of the minimum nighttime temperature may be as high as 4.0°C [11, 12], combined with a significant increase in exposure to heat waves and ground-level ozone [13, 14]. As a result of the combined significant increase of the planetary and urban temperature, and considering the substantial increase of the global population and the socioeconomic trends in the building sector, it is forecasted that the buildings cooling energy consumption will increase between 250–1000% with the range depending on the global economic and technological developments [15].

To counterbalance the impact of urban overheating, advanced and efficient heat mitigation technologies must be implemented at the city scale. Recent heat mitigation research has provided innovative and efficient technologies that decrease the temperature of the cities substantially [16]. It is reasonably expected that the development of advanced materials for buildings and urban structures, including photonic passive daytime radiative coolers (which can achieve sub-ambient surface temperatures) when combined with optimised greenery solutions (which can provide substantial evapotranspiration rates under high ambient temperatures) can substantially mitigate urban heat [17–21].

As buildings are responsible for about one-third of global energy consumption, improving building energy efficiency offers a significant opportunity to make cities more sustainable environments [22]. It is, thus, important to evaluate the current energy use in cities, investigate strategies to reduce energy use and environmental impacts, and assess building retrofit opportunities. To estimate urban building energy demand, urban building energy modelling (UBEM) is necessary to analyse the dynamic and complex interdependencies between urban buildings and the urban environment [22]. It requires simulation and optimization to account for interactions among buildings and between buildings and their surrounding urban areas. A cooler surrounding environment reduces cooling loads in urban buildings and increases efficiency of cooling systems, which combined can reduce anthropogenic heat from buildings to the ambient [23]. UBEM, thus, allows designing and operating urban buildings from a city block to a district or an entire city rather than as single individuals.

Very little is known about the potential contribution of the newly developed innovative heat mitigation technologies on the climate of cities, the expected heat mitigation potential, and their capacity to reduce the cooling energy consumption of urban buildings. Studies assessing the heat mitigation potential of conventional reflecting materials show that it is rational to achieve a drop of the peak ambient temperature up to 1.5°C [23] and a decrease of the cooling energy demand at the city scale between 15 to 35%, as a function of the local climatic characteristics and the quality of the building stock [24, 25].

It is expected that the implementation of the new generation of photonic materials will contribute to a higher urban temperature drop and a substantial increase in the cooling energy benefits. Given the limited number of large-scale heat mitigation projects implemented in cities and the absence of detailed assessment studies, there is a serious lack of knowledge about the exact climatic contribution of each of the newly developed innovative heat mitigation technologies and their potential combined implementation in cities. In parallel, there is a complete lack of data and information on the energy impact of a large-scale implementation of these technologies at the city scale.

The present article presents the methodology, characteristics, and results of the largest, to our knowledge, world urban heat mitigation project designed for the city of Riyadh, Saudi Arabia. It is the first time that a) the most advanced and the newly developed heat mitigation technologies and their combination are assessed using advanced climatic modelling for the whole urban area, and b) the cooling energy potential of the considered technologies is evaluated for a very high number, 3323, of existing urban buildings using advanced energy simulation techniques. To our knowledge, it is the first time that the climatic and energy impacts of such a large-scale heat mitigation project are evaluated, analysed and presented.

This paper delves into the compelling relationship between urban heat mitigation and energy conservation, exploring the various strategies employed to counter the rising temperatures in cities and their substantial contributions to promoting energy efficiency, sustainability, and overall urban resilience. Through a comprehensive analysis of the multifaceted impacts of mitigating urban heat, this study sheds light on the pivotal role such measures play in creating more liveable, energy-efficient urban environments for current and future cities. We believe that the article will contribute substantially to properly designing heat mitigation studies in cities, assess their energy potential, and contribute to improved living conditions, sustainable urban development, and urban resilience.

2. Results

Riyadh, the capital of Saudi Arabia, has a hot desert climate, 'Bwh', based on the Köppen-Geiger climate classification system [26]. Ambient temperature during the summer period may reach 45°C, skyrocketing the cooling energy consumption of buildings.

2.1 Current Climatic Conditions

The magnitude of the UHI in Riyadh is persistent and well-captured by the network of stations. The temperature distribution is rather regular, with almost no outliers and high daily average temperatures exceeding 40.0°C in the city. The differences between urban and reference contexts are systematic and stable, with frequent peaks exceeding 4.0°C and differences nearing 1.8°C for 75% of the examined period (3rd quartile) and a median of 1.2°C (Figure S6 (b)). Negative values, namely when the city is cooler than the surroundings, are rarely computed (Figure S6 (a)). Additional information on the climatic analysis is given in Supplemental Information 1.

The cooling degree days in Riyadh are quite consistent over the observed period, with very high values, exceeding 2000 at all locations (Figure S7) excluding stations 1 and 4, Table S2, where the four-year average CDDs exceed 1850 and 1800, respectively. The CDDs at urban locations are approximately 280 higher than those at reference locations (computed as the difference between urban and reference averages, considering the five-year average). The five-year average of the CDDs at reference (background non-urban) locations is equal to 1960, while it is 2236 at urban locations. This 14% increase in CDDs in the city with respect to the reference locations is in line with the literature [6], which states an average increase of 13%. However, even within the city, there is a difference of 160 CDDs between the hottest (Al Amal, 2291 CDDs) and the coolest urban area. These important intra-urban and urban-reference differences point out the influence of local factors (such as land cover and wind patterns), with the potential to exert a strong influence on the cooling energy performance of buildings.

The analysis as performed on the integrated data set (ground and simulated data) has resulted in the following results/conclusions.

- a. During the hottest conditions and considering all urban cells/data points, more than 50% of air temperature data exceeds 40.0°C, and 10% of the urban area has air temperature higher than 45.0°C. In contrast, on an average summer day, only 23% of the urban cells/data points have air temperatures exceeding 40.0°C, whereas air temperature does not exceed 45.0°C. This result shows that in the hottest climatic conditions, hot spots are not limited, and a considerable number of urban areas experience high ambient temperatures.
- b. The average UHI intensity of the entire urban area during the summer period, as predicted by the mesoscale model, is 1.5°C, Figure S12. The southern and eastern parts have the highest UHII with an average intensity of more than 2.0°C and the highest average value of 2.5°C. The mean UHI intensity increases with the increase of urban density. The mean UHI intensity corresponding to low-density urban cells exceeds 2.0°C for 6% of the time. In medium-density and high-density areas, the corresponding percentages of time when UHI intensity exceeds 2.0°C are 24.6% and 36.6%, respectively. This pattern of UHI with respect to the urban type is similar to the pattern of air temperature in relation to the urban type. These figures are consistent with the observations from the network of weather stations.

- c. The maximum calculated daytime UHI intensity in the whole city was close to 8.5°C and appeared at 14:00, Figure S13. The southeastern part of the city experienced high UHI intensity with a magnitude of above 8.0°C, Figure S13. It is observed that the UHI intensity and air temperature are closely related between 8:00 am and 8:00 pm. Outside this time range, the UHI intensity has a stronger relationship with the wind direction. The maximum UHI intensity was calculated to occur during northern winds, while the minimum intensity corresponded to southern and southwest winds.
- d. Land surface temperature (LST), in the greater Riyadh urban zone, presents a significant variability. Up to 5.0°C, higher average surface temperatures are observed in the south and southeastern parts of the city, Figure S10. LST in Riyadh obtains values higher than 50.0°C during summer months in all its districts, whereas districts in the northeast and the southeast of the city exhibit LSTs even higher than 58.0°C. This is an important finding as land surface temperature a) drives the transfer of heat from the ground to the overlying air and thus contributes to higher air temperatures, at least at levels close to the ground, and (b) reduces soil humidity. The land surface temperature at 14:00 ranges between 46.1°C and 53.3°C. Additional data about the distribution of the LST in the city is obtained through the Landsat 8 satellite Observations at 10:30 am local time per district was used to reveal using the QGIS software, the most thermally stressed districts of the city. Figure S14 shows the distribution of the mean daily land surface temperature per district during a hot day as calculated by the mesoscale simulations.

High temperatures in urban areas have a direct impact on human health and are associated with heat-related stress and excess summer deaths [27]. We assessed the distribution of the urban heat risk in the city based on the collected and calculated meteorological characteristics expressing the degree of heat exposure, namely the physical characteristics and in particular, the urban planning characteristics that indicate the way the city has been built and the way it operates (building materials, buildings age, number of public facilities, etc), and the social characteristics involving demographic characteristics expressing the degree of sensitivity to extreme hot weather conditions estimated by census data such as the percentage of population over 65 or under 14 years old. For example, districts exhibiting high temperature values, low quality building structures and are inhabited by a high percentage of elderly people are more vulnerable to extreme heat than districts characterized by lower temperature values, high quality buildings and their population consists of younger people.

To assess the heat risk of Riyadh, the parameters presented above were combined into a composite heat risk indicator. To achieve this, each parameter was reclassified into three categories using the quantile classification, namely a data classification method that distributes a set of values into groups that contain an equal number of values. Table S3 provides the range of values for the three risk categories per parameter [28, 29]. The resulting three categories are defined as: 1) Low heat risk, 2) Moderate heat risk, and 3) High heat risk. Since the relative importance of each parameter is unknown, all parameters contributed equally to the composite heat risk index. The sum of all parameters was then reclassified into three categories using the quantile classification method, resulting in the composite heat risk index (Figure 1). It yields that the northeast and southeast districts of the city (in red) have higher heat risk than those to the west of the city. Several districts in the centre of the city are also exhibiting high thermal risk.

2.3 Design of The Mitigation Strategy

The detailed analysis of the current climatic and heat risk conditions in Riyadh reveals that the main axes of the potential interventions to mitigate urban heat in Riyadh should aim to: a) decrease the surface, LST, and ambient temperature and reduce the heat advection from the surrounding desert, b) reduce the strength of the sensible heat in the city, c) surge the magnitude of latent heat, d) improve solar control in the city, and e) decrease the levels of the released anthropogenic heat as much as possible.

We designed and evaluated, in detail, eight mitigation scenarios focusing on the above objectives. A short description of the scenarios is given in Table 1. To decrease the surface temperature in the city and reduce the release of sensible heat, reflective materials as well as super cool materials consisting of passive daytime radiative cooling coatings are considered. Reflective materials are commercially available and present a high reflectance to solar radiation and a high broadband emittance and contribute to reducing the surface temperature up to 10.0°C [30]. Super cool materials, (SCM), or photonic

daytime radiative cooling coatings, or are recently developed and gradually penetrating the market. Super Cool Coatings exhibit sub-ambient surface temperatures and depending on the local climatic conditions can reduce the surface temperature of cities up to 15.0°C [18]. By lowering the surface temperature in the city, the height of the planetary boundary layer may decrease, resulting in reduced heat advection from the desert [31].

An increase in the green infrastructure in cities provides solar control and helps to decrease the release of sensible heat, while it highly enhances the release of latent heat in the city through evapotranspiration processes [20]. The cooling efficacy of urban greenery under high ambient temperatures, like in Riyadh, depends highly on the proper provision of irrigation [32]. Above a threshold ambient temperature and under low watering conditions, the magnitude of evapotranspiration of greenery is reduced significantly, while the released Biogenic Volatile Compounds, BVOCs, may surge, resulting in serious air quality problems [33].

Combined scenarios considering the implementation of both reflective or super cool materials with additional irrigated or non-irrigated greenery are designed and evaluated through mesoscale climatic modelling. Table 2 provides the calculated cooling performance and the corresponding mitigation potential regarding the ambient and surface temperatures for the eight scenarios. In addition, Table S2-1 provides the calculated average values of the Mean, Maximum and Minimum values of the main climatic parameters for the reference and the 8 mitigation scenarios, while Table S2-2 presents the number of hours that the average temperature in Riyadh is above a threshold ambient temperature as well as the corresponding value of the Cooling Degree Hours for the reference case and the eight mitigation scenarios during the whole summer period.

Analysis of the performance of the eight mitigation scenarios leads to the following main findings:

- a. An almost linear association between the reference temperature (no mitigation) and the potential temperature decrease is observed for both day and night periods. In general, and for all the mitigation scenarios, the higher the background temperature, the higher the potential temperature decrease. Figure S2-1 demonstrates the relation of the background temperature with the temperature drop for both the day and night and for the scenario 'Very Reflective Riyadh'.
- b. The implementation of the super cool materials on the roofs of the buildings, combined with well-irrigated additional greenery, offers a higher mitigation potential and contributes to the reduction of the average 24 h ambient temperature in the city between 1.3°C to 7.5°C with an average value close to 4.2°C. The corresponding decrease of the ambient temperature at 2:00 pm varies between 0.0°C to 3.0°C, with an average value close to 1.4°C, while at 6:00 am the change of ambient temperature varies between an increase of 2.8°C and a decrease of 8.6°C, with an average decrease close to 3°C. In parallel, the reduction of the surface temperature in the city at 14:00 pm varies between 3.5°C to 7.3°C with an average value close to 4°C. During the whole summer period, the decrease of the overheating hours above 35°C and 40°C is 23.1% and 29.4%, respectively, while the decrease of the Cooling Degree Hours, CDH, base 35°C and 40°C is 28.4% and 47.6% respectively.
- c. Moderate increase of the low-level non-irrigated greenery at the city scale has a limited capacity to cool the city during daytime, 2:00 pm, while it may even increase slightly the temperature. The top layer soil moisture decreases during the summer because of the lack of precipitation during the summer period. By increasing the vegetation cover, the moisture level continues to decrease because of the larger surface of evapotranspiration. Under such soil moisture conditions, low-level vegetation with shallow roots can no longer evaporate effectively and plants cannot release latent heat, resulting in a very limited decrease or even increase of the daytime ambient temperature. Similar results were reported in [34] for Los Angeles, where it was demonstrated that adding and replacing existing plants in the city with drought-tolerant plants without additional irrigation water prevents plants from effectively helping the city to relieve UHI and heat wave conditions. During the night, the cooling contribution of low-level non-irrigated greenery is more significant as plants reduce the upward heat flux from the ground, resulting in a cooler soil surface at night. The average nighttime temperature decreases as caused by low-level non-irrigated greenery may reach 3.0°C. This is in full agreement with many other similar studies reporting the cooling potential of additional greenery in cities [35].

- d. A significant increase in the cooling potential of additional urban greenery is observed when high-level irrigated trees are considered. The average ambient 24 h temperature is found to decrease between 0.4°C and 7.2°C with an average value close to 3.5°C. The corresponding average decrease of the ambient temperature at 2:00 pm and 6:00 am is 0.6°C and 2.1°C, respectively. In parallel, the overheating hours above 35.0°C and 40.0°C decrease by up to 19.1% and 14.1%, respectively, while the corresponding decrease of the cooling degree hours is 17.1% and 21.5%, respectively.
- e. Although non-irrigated vegetation shows a cooling effect at night, they are not effective in reducing CDHs during the daytime. Non-irrigated vegetation leads to slightly higher CDHs compared to the reference scenario when the base temperature exceeds 38.0°C, while irrigated vegetation reduces CDHs during the day. Shading and evapotranspiration contribute most to the cooling effect of vegetation under greenery scenarios. The denser the plant canopy, the higher the cooling potential, as long as plants are sufficiently supplied with water for transpiration. However, the cooling potential of trees and other vegetation is severely reduced under dry conditions when soil water is limited, which results in drought stress to the plants and lower evapotranspiration. The variation of the CDHs during the day and night-time for different base temperatures, as well as for all the considered scenarios, is shown in Figure S2-2.
- f. An increase of the urban albedo contributes to the decrease of the peak daytime ambient temperature between 0.2°C and 2.2°C with an average value close to 1.2°C, while the daily average decrease of the urban surface temperature is close to 4.8°C. Reflecting materials decrease the CDHs with base temperatures of 35.0°C and 40.0°C, by 19.5% and 47.6%, respectively, while the corresponding decrease of overheating hours is 7.0% and 24.1%.
- g. Implementation of super cool passive daytime radiative cooling materials on the roofs of urban buildings presents a very significant heat mitigation potential. They decrease the peak ambient temperature at 2:00 pm between 0.3°C to 2.3°C with an average value of 1.3°C, while the corresponding decrease of the urban surface temperature is 6.6°C. Super cool materials contribute to the decrease of the CDHs with the base temperatures of 35.0°C and 40.0°C, by 21.9 % and 50.8%, respectively, while the corresponding decrease of the overheating hours is 8% and 28.1%. Given the very high reflectance of the super cool materials, their use should be limited on the roof of buildings to avoid optical annoyance problems. The development of coloured daytime radiative cooling materials presents a much lower reflectance but a quite similar cooling potential because of the addition of fluorescent components, which will extend the applicability of SCM's in building facades and pavements and will boost their cooling capacity in cities.

2.4 Impact of Heat Mitigation Technologies on the Cooling Energy Consumption of Buildings

Using the CityBES simulation platform, the cooling energy consumption of 3323 buildings located in the Al Masiaf precinct of Riyadh is evaluated for the whole summer period using weather files corresponding to the current climatic conditions as well as to the eight designed mitigation scenarios. The simulated buildings consist of residential and commercial buildings of 1 to 4 storeys.

The average summertime cooling load of all the buildings, COP=1, is 104.6 kWh/m². The total summertime cooling load of all buildings is 222. 3 GWh. As expected, the taller the building, the lower the cooling load. The calculated average load for the one, two, three and four-storey buildings was 122.1 kWh/m², 103.3 kWh/m², 103 kWh/m² and 88.2 kWh/m², respectively (Figure 2).

The calculated average summertime cooling load corresponding to the eight mitigation scenarios is given in Table 3. Calculations for all cases are performed using the same building characteristics considered in the reference scenario, Table S1, and the albedo of the buildings has not been modified. Thus, the reduction of the cooling load is due only to the decrease of the ambient temperature caused by the mitigation technologies and not to the lower absorption of solar radiation by the structure of the building.

As shown, the mitigation scenarios investigated here result in a decrease in the average summertime cooling, with the reduction ranging between 3.6% and 16%. The use of high albedo and supercool materials (Reflective and Very reflective scenarios) reduces the cooling load by 4.4% and 5.2% compared to the reference scenario, respectively. The Green and Dry

and the Very Green and Dry scenarios lead to a decrease of 3.9% and 10.6% of the average summertime cooling loads compared to the reference condition, while this reduction is slightly higher once considering the irrigated vegetation (i.e., 5.4% and 13.4%, respectively). The combination of Very Reflective and Very Green with the non-irrigated vegetation scenario shows a 14.8% reduction in the average cooling loads compared to the reference scenario. The maximum reduction of 16.0% in the average summertime cooling load is achieved by the combination of Very Reflective and Very Green with the irrigated vegetation scenario. Therefore, the implementation of heat mitigation technologies in the considered urban area can provide a reduction of the cooling load up to 35.5 GWh during the summer period. Figure 3 demonstrates the distribution of the annual cooling load in the study area for the eight investigated mitigation scenarios.

The energy conservation potential of the mitigation technologies implemented on the façade or roof of the buildings is considerably increasing when the direct benefits arising from the reduction of the absorbed solar radiation are considered. Tables S2-3 present the potential cooling load reduction in buildings of one to four storeys under the reflective and very reflective mitigation scenarios, considering both the direct and indirect benefits arising from the implementation of the reflective and super cool materials on the roof of the buildings. Under the reflective scenario, when the decrease of the absorbed solar radiation is considered, the cooling load conservation increases on average from 4.4% to 5.6%. Under the very reflective scenario, the cooling load conservation increases from 5.2% to 6.9%. In absolute values, the total cooling load reduction in the urban area under the reflective scenario will rise from 9.8 GWh to 12.4 GWH, while for the very reflective scenario, the corresponding reductions are 11.6 GWh and 15.3 GWh. The calculated reductions indicate that for both scenarios, almost 75% to 78% of the potential conservation of the cooling load in the 3323 buildings is attributed to the decrease of the ambient temperature induced by the implementation of the mitigation technologies at the city scale, underlying the energy conservation impact and consequently the considerable decarbonisation potential of urban heat mitigation technologies.

Energy retrofitting of buildings is the most efficient way to decrease their energy demand. To evaluate the importance of the combined impact of energy retrofitting and heat mitigation technologies implemented at the building and city scale, respectively, we designed and simulated the energy impact of building retrofitting measures for all the 3323 buildings combined with heat mitigation technologies implemented at the urban scale. The energy retrofitting measures mainly included measures to improve the thermal quality of the envelope, namely better windows, better insulation, improved solar control, cool roofs, and improved air permeability. Measures related to the HVAC system are not considered. A full list of the selected energy retrofitting measures is given in Table S2-4.

The calculated reduction of the summer cooling load in the urban area, considering the combined implementation of the heat mitigation and energy retrofitting measures (Q_{comb}) as well as the corresponding cooling benefits (Q_{mit}) when only mitigation measures are considered, are given in Table 4 for all the scenarios. Given the important thermal interaction between the energy retrofitting and the heat mitigation measures during the building operation, the difference between $Q_{\text{comb}} - Q_{\text{mit}}$ does not represent the exact contribution of the retrofitting measures and is lower than when retrofitting measures are applied individually. Simulation of the energy impact of the retrofitting measures under non-mitigated climatic conditions is also performed for all the buildings, and the corresponding reduction of the cooling load of the reference building is calculated (Q_{retr}). However, under the combined implementation of the mitigation and retrofitting measures, the real contribution of the heat mitigation and energy retrofitting measures are lower than Q_{mit} and Q_{retr} , respectively, because of the important thermal interaction between the considered measures. Nevertheless, a comparison between Q_{mit} vs Q_{comb} and Q_{retr} vs Q_{comb} can provide an approximate but quite realistic contribution of the mitigation and retrofitting technologies. As shown in Table 4, combined heat mitigation technologies can contribute up to 46% of the total cooling load conservation of urban buildings under the combined implementation of heat mitigation and energy retrofitting measures.

3. Discussion

The temperature of cities is steadily increasing and is expected to increase further in the future because of the intensive urbanisation, overpopulation, and global climate change [11]. Urban overheating has a serious impact on urban life highly affecting the energy sector by increasing the cooling consumption and the peak electricity demand [5]. To lower urban air and surface temperatures and counterbalance the impact of high temperatures on the energy demand for cooling, heat mitigation technologies have been developed and implemented [36]. While the impact of conventional mitigation technologies like the use of conventional reflective materials or urban trees and greenery is assessed for several cities, there are important knowledge gaps regarding the mitigation potential of advanced technologies like the photonic daytime radiative cooling materials, the specific impact of irrigated or non-irrigated greenery, and the combined effect of materials and greenery as well as on the energy impact of heat mitigation at the urban scale.

The study underscores the critical importance of mitigating urban heat as a multifaceted approach to conserving energy in cities. The integration of green infrastructure, technological advancements, and community involvement demonstrates the potential to significantly reduce energy consumption associated with cooling systems and create more resilient, sustainable urban environments. This synergy not only addresses the immediate challenges of urban heat but also aligns with broader goals of energy efficiency and environmental stewardship.

This paper presents the first study, to our knowledge, investigating the large-scale energy benefits of advanced and conventional single and combined heat mitigation technologies implemented at the city scale. The results shown here provide necessary data to mitigate urban heat and reduce energy use in urban settlements based on interactions between urban building energy demand and the urban climate.

Increase in the green infrastructure in cities is the most commonly considered mitigation technology. We show that the main driver for cooling is to improve the transpiration efficiency of plants used to mitigate urban heating, so they can reduce the released sensible heat and increase the flux of latent heat flow. Various plant species show different transpiration rates, while individuals of the same species may reveal transpiration rate variations depending on the prevailing environmental conditions [37]. Transpiration can normally evaporate water from 0.28 to 12 L/m² per day [42], thus generating a cooling power ranging between 24.5 and 29.5 MJ/m² per day in arid environments with sufficient water supply; however, it is less than 10 MJ/m² in temperate climate [33]. Irrigation has a significant role in urban cooling [38, 39], as it enhances the performance of greenery by increasing evapotranspiration [40]. In the absence of irrigation, evapotranspiration cannot be effectively stimulated. As a result, the scenario with higher vegetation coverage (60%) could perform even worse than the lower coverage scenarios. Furthermore, the dry soil conditions prevent plants from effective evapotranspiration during the day, and most of the contribution to the latent heat flux during the day comes from direct soil evapotranspiration. The results from the irrigated scenarios show that irrigation is a key factor in achieving an appreciable mitigation effect for vegetation-based mitigation strategies in Riyadh and other hot arid cities. The daytime transpiration of both the low-rise vegetation (shrubs and grass) and high-rise vegetation (broadleaf trees) is strongly enhanced by introducing irrigation.

Irrigated greenery presents a considerable mitigation potential, especially during nighttime. This is in agreement with most of the existing studies assessing the cooling potential of greenery [35]. It is found that, on average, the irrigated greenery in the city may decrease the peak daily temperature up to 0.7°C and the nighttime temperature up to 2.1°C. This agrees with similar studies reported in [35, 41-43].

High urban temperatures affect the physiological processes of greenery and their transpiration capacity, resulting in a much lower cooling potential [44]. Excessive temperatures usually combined with drought, result in the closure of the plant stomates, senescence and increase of the leaves temperature above the ambient one and disruptions to the plants nutrient system [45]. The increase of the surface temperature of the plants increases the release of sensible heat and may result in heating of the ambient air [20]. Several mechanisms are used by plants to ameliorate part of the thermal damage like the increase of the reflectance of the leaves to decrease the absorption of solar radiation and the production of heat shock proteins [46]. Watering is the most efficient way to protect plants and avoid ambient heating. Experiments have shown that well-irrigated plants maintained their sap flow during heat waves, while non-irrigated plants reduced their sap flow by

50% [47]. However, literature reports that some species can keep their stomata open under extreme ambient temperatures and provide transpirational cooling; however, very little is known on the topic [48]. Horticultural research aims to develop more heat-tolerant species using several breeding protocols. Currently, genetic plants engineering has progressed up to the point at which genes of proper traits are introduced and expressed efficiently [49].

Apart from the climatic impact, urban greenery strongly affects the urban environmental quality. Trees, contribute to decreasing the concentration of harmful pollutants like ground-level ozone and Particulate Matter [50]. Trees can remove between 2-7% of the locally emitted PM₁₀ [51], while can reduce the 8-hour average peak concentration of PM₁₀ by 1-2% [52]. However, trees emit BVOCs, which are about 2-3 times more reactive than the average emissions of oil combustion [53]. The majority of BVOCs are isoprenoids, monoterpenes and sesquiterpenes, which result in a considerable increase in the concentration of tropospheric ozone and the production of airborne particles during periods of high temperature [54].

Although numerous articles have investigated the impact of urban greenery on reference or representative buildings, very few studies have assessed the energy benefits at the city or neighbourhood levels [55-65]. In addition, even though existing articles reflect high non-homogeneity regarding the considered urban climate, levels of urban overheating, type and magnitude of greenery, quality of buildings and assessment methodology, important conclusions can be drawn:

A) The 24 h average temperature decrease induced by additional urban greenery is found to vary between 0.2 to 2.5°C. Most of the articles report an average 24 h temperature drop between 0.7°C and 2.2°C without specifying the irrigation status of the greenery. In the present study, a moderate rise of urban greenery, (30%), decreases the 24 h ambient temperature between 0.7°C (non-irrigated) and 1.2°C (irrigated), while a high increase of the green infrastructure, (60%), results in a temperature decrease between 2.3°C and 3.5°C.

B) Almost all previous studies agree that most of the cooling benefits from urban greenery occur during night-time. Most of the studies report that the temperature decrease during the peak daytime period is between 0.0°C to 1.0°C with a mean value close to 0.4°C. Almost all studies are performed for temperate climates and non-arid urban zones except [34], which reported a relative increase in the ambient temperature when non-irrigated plants are considered. Similar results are obtained in the present study for non-irrigated plants, while the peak temperature decrease varied between 0.3°C and 0.6°C when irrigation is considered.

C) The potential decrease of the cooling load induced by urban greenery is reported by very few articles. A direct comparison is almost impossible given the different climatic conditions, building stock and characteristics of the considered additional greenery. Annual cooling energy conservations varying between 2 to 14 kWh/m² are reported, close to the results of the present study for non-irrigated greenery, 4 kWh/m² and 11 kWh/m², and 5.7 kWh/m² to 14 kWh/m² for irrigated greenery.

The increase of the urban albedo by the implementation of reflective materials contributes to the decrease of the absorbed solar radiation and reduces the urban surface temperature and the release of sensible heat. Up to the present time, two types of reflective materials, white materials, and coloured infrared reflective coatings, have been developed and implemented in cities in the form of cool roofs or cool pavements [36, 66]. The new generation of reflective materials based on nanotechnological additives like thermochromic coatings, or PCM doped paints, have been developed without however to achieve a considerable penetration to the market [67 68]. Previous studies evaluating the potential impact of modified albedo in cities by using mesoscale climatic modelling reported a range of the 24 h decrease of the ambient temperature between 0.1°C and 0.8°C, and a peak daily temperature reduction between 0.5°C to 3.5°C, with the variation depending on with the characteristics of the cities and the implemented albedo scenario [23, 69]. In general terms, it is found that an increase of the albedo by 0.1 results in a decrease of the ambient temperature close to 0.18°C in the afternoon (5 pm) [69]. The present study found that the average 24 h as well as the peak daily temperature decrease are 0.9°C and, 1.2°C respectively, in full agreement with the previous findings.

The recently developed super cool or daytime radiative cooling materials present a very high solar reflectance value combined with high emittance at the atmospheric window, while they have not yet been implemented to mitigate urban

overheating. Mesoscale simulations for the city of Kolkata, India, have shown that super cool materials may contribute to decreasing the peak temperature of cities up to 4.5°C, imposing, however, a considerable heating penalty during the winter period [70]. Modulation of their optical properties, mainly reflectance and emittance, to reduce the strength of cooling during the cold period could minimize the problem [71, 72]. Simulations have shown that optically modulated super cool materials can maintain their summer cooling capacity while contributing to increasing the winter ambient temperature up to 1.5°C [73]. The present study has found that the average 24 h as well as the peak daily temperature decrease are close to 0.9°C and 1.3°C, respectively. The specific values are lower than those reported for the city of Kolkata as the implementation of the super cool materials is considered only for the roofs of the buildings and not for pavements and the other surfaces of urban buildings. Given the extreme reflectance of the materials, implementation at low levels structures can create important glare and contrast problems. A new generation of coloured super cool materials presenting a much lower solar reflectance, but a similar cooling potential is expected to boost the implementation of these materials in cities. Such materials compensate for the decrease in the solar reflectance with fluorescent components that present important cooling potential [74].

Although important recent advancements have been achieved in heat mitigation research, significant challenges remain, and future studies need to be developed focusing on warming climate, mitigation and adaptation technologies, energy use, and the correlation between urban human mobility and urban building energy consumption. The UBEM analysis offers vital information to support city planners in city-scale energy retrofit programs. Thus, simulations of UBEM, existing building energy datasets, and computing challenges can be further promoted for wider applications and coupling the urban microclimate model with UBEM to evaluate and prioritize mitigation measures that can cool the urban environment while reducing cooling loads in buildings.

The multifaceted strategies employed to mitigate the adverse impacts of UHIs not only alleviate the discomfort caused by excessive heat but also contribute significantly to the broader goals of sustainable urban development and reduced energy consumption.

The findings emphasize the effectiveness of various urban heat mitigation techniques in curbing energy usage. Green infrastructure, such as vegetation and reflective surfaces, provides natural cooling mechanisms that lessen the demand for energy-intensive cooling systems. These measures translate to lowered electricity consumption, reduced carbon emissions, and increased energy efficiency, contributing to the overall sustainability of urban areas.

Moreover, the integration of technological advancements and smart solutions emerges as a critical catalyst for energy conservation. Automated cooling systems, real-time data monitoring, and adaptive energy management demonstrate the potential to optimize energy consumption while maintaining comfortable living conditions. These innovations align with the modern concept of smart cities, where technology is harnessed to create urban environments that are both liveable and environmentally conscious.

The significance of community engagement and awareness cannot be understated. When residents are informed about the benefits of urban heat mitigation and their role in energy conservation, they become active participants in creating more resilient and energy-efficient cities. This collaborative effort reinforces the positive impact of these strategies and fosters a sense of ownership in shaping a sustainable urban future.

While the benefits are evident, challenges such as initial costs, implementation logistics, and the need for comprehensive urban planning require careful consideration. Striking a balance between short-term investments and long-term energy savings is essential in steering urban development toward a more sustainable trajectory.

4. METHODS

We designed a research methodology including three main tasks as described in the Methods Chapter. First, a detailed mesoscale simulation of the climatic conditions in the city is performed and validated against extensive existing climatic data. In essence, model results validation is a critical step that underpins the credibility and utility of modelling efforts. It

transforms models from theoretical constructs to practical tools that can inform, guide, and drive meaningful real-world outcomes. Further to its validation, the mesoscale model is used to populate the climate data of Riyadh at improved spatial resolution to obtain a more complete view of spatial and temporal trends and differentiations. In the second stage, based on the analysis of the climatic conditions, eight heat mitigation strategies and the corresponding scenarios were designed and evaluated in terms of their performance using mesoscale climatic modelling. Finally, detailed precinct scale cooling energy simulations are performed for the Al Massiaf central area, including 3323 urban buildings. Energy simulations are performed under the current climate as well as under the modified climatic conditions corresponding to the eight heat mitigation strategies, Figure 4.

Climatic simulations are performed using the Weather Research and Forecasting (WRF) model, Version 4.2.1 [75]. The simulation domain was centred on the city of Riyadh, and three one-way nested domains with horizontal resolutions of 4.5 km, 1.5 km and 0.5 km were used, where the innermost domain was Riyadh city. The outer two domains were used to provide boundary conditions for the innermost domain (Figures S1 and S2). Supplemental information 1 provides detailed information on the implementation of the Weather Forecasting Model. The developed mesoscale model was used to calculate the hourly distribution of the main climatic parameters for the entire summer in the city of Riyadh under the existing conditions and the eight mitigation scenarios. The hourly outputs from the nearest grid close to Al-Masiaf precinct are used to create nine weather files for the purpose of energy simulations representing the reference climate conditions and all mitigation scenarios. The results obtained from the reference scenario mesoscale simulation were validated against the observations from three existing weather stations to ensure the performance of the model. Validation has been performed for both the summer and winter periods and for the most important climatic parameters, ambient temperature, wind speed and relative humidity. We obtained a satisfactory agreement between the simulated and experimental data. In particular, the simulation results slightly overestimated the wind speed, which could result from the underestimation of building heights. Details of the validation exercise are given in Supplemental Information 1. Figures S3 and S4 present the simulated and experimental data for the three stations.

The 3323 buildings selected for cooling energy simulations are located at the Al Masiaf Precinct, which covers an area of approximately $2 \text{ km} \times 2 \text{ km}$ (Figure S5) with a total of 3323 buildings, including residential buildings (2962 multi-family and 98 single-family houses) and office buildings (241 small, 21 medium, and 1 large offices). The total area of the selected buildings to simulate is 2125820 m^2 .

The simulation platform CityBES [76, 77] was used to run the energy simulations of the Al-Masiaf precinct. CityBES is a web-based data and computing platform developed by Lawrence Berkeley National Laboratory (LBNL) to evaluate the energy performance of city buildings. Figure 5 shows the key components of CityBES as organised in three layers: 1) the data layer, 2) the simulation engine (algorithm) and software tools layer, and 3) the use-cases layer. CityBES [76, 77] offers detailed energy performance analysis built on the EnergyPlus engine for dynamic energy simulation of urban buildings, which offers the highest resolution due to physics-based modelling approaches capturing the full dynamic of building performance [30]. Specific information and details about the specific simulation procedure are given in Supplemental Information 1. The most common construction and operational characteristics of the residential and commercial buildings in the Al Masiaf precinct are identified and then used to perform the building energy simulations. Table S1 lists all the main inputs used to simulate the residential and commercial buildings.

To analyse the current climatic conditions in the city, data from a network of 16 meteorological stations is used (Table S2). The dataset analysed comprises the five recent complete years of hourly averages of data from January 2016 to December 2020 representing the current conditions in the city. A detailed statistical methodology described in the Supplemental information was used to filter the data and control their quality.

We calculated the magnitude of the urban heat island in the city by considering the difference between a reference (non-urban) station and an urban station where the reference data was obtained from the average of four meteorological stations located at all four sides of the city, in this way, a reliable appraisal of the differences between the city and the non-urban

surroundings is achieved. The difference is calculated considering the simple moving average over seven hours (3 hours backwards, and 3 hours forward and centred on the hour). This approach eliminates short-term differences due to atmospheric circulation conditions and better captures the general trends over the day, as performed in [78].

The climatic information provided by the ground stations was enriched with additional data regarding the spatial distribution of the main climatic parameters, the hottest spots in the city, and the distribution of the latent and sensible heat fluxes as calculated by mesoscale simulations under the current climatic conditions. The calculated spatial distribution of the ambient and surface temperature, wind speed, UHI intensity and sensible and latent fluxes are provided in the supplemental information, Figures (S8-S13).

Declarations

Acknowledgement

Authors acknowledge the Royal Commission of Riyadh to support the project "Strategic study on urban heat and mitigation potential in Riyadh - KSA Cooling Riyadh".

References

1. Oke, T.R., *The energetic basis of the urban heat island*. Quarterly journal of the royal meteorological society, 1982. **108**(455): p. 1-24.
2. Founda, D. and M. Santamouris, *Synergies between Urban Heat Island and Heat Waves in Athens (Greece), during an extremely hot summer (2012)*. Scientific reports, 2017. **7**(1): p. 10973.
3. Tuholske, C., et al., *Global urban population exposure to extreme heat*. Proceedings of the National Academy of Sciences, 2021. **118**(41): p. e2024792118.
4. Santamouris, M., *Analyzing the heat island magnitude and characteristics in one hundred Asian and Australian cities and regions*. Science of the Total Environment, 2015. **512**: p. 582-598.
5. Santamouris, M., *Recent progress on urban overheating and heat island research. Integrated assessment of the energy, environmental, vulnerability and health impact. Synergies with the global climate change*. Energy and Buildings, 2020. **207**: p. 109482.
6. Santamouris, M., *On the energy impact of urban heat island and global warming on buildings*. Energy and Buildings, 2014. **82**: p. 100-113.
7. Santamouris, M., et al., *On the impact of urban heat island and global warming on the power demand and electricity consumption of buildings—A review*. Energy and buildings, 2015. **98**: p. 119-124.
8. Bartos, M., et al., *Impacts of rising air temperatures on electric transmission ampacity and peak electricity load in the United States*. Environmental Research Letters, 2016. **11**(11): p. 114008.
9. Bloomberg. *Bloomberg Green Newsletter*. 2022; Available from: <https://www.bloomberg.com/green>.
10. Hamdi, R., et al., *Assessment of three dynamical urban climate downscaling methods: Brussels's future urban heat island under an A1B emission scenario*. International Journal of Climatology, 2014. **34**(4): p. 978-999.
11. Zhao, L., et al., *Global multi-model projections of local urban climates*. Nature Climate Change, 2021. **11**(2): p. 152-157.
12. Oleson, K., *Contrasts between urban and rural climate in CCSM4 CMIP5 climate change scenarios*. Journal of Climate, 2012. **25**(5): p. 1390-1412.
13. Wang, Y., et al., *Future population exposure to heatwaves in 83 global megacities*. Science of The Total Environment, 2023. **888**: p. 164142.
14. Jiang, X., et al., *Predicted impacts of climate and land use change on surface ozone in the Houston, Texas, area*. Journal of Geophysical Research: Atmospheres, 2008. **113**(D20).

15. Santamouris, M., *Cooling the buildings–past, present and future*. Energy and Buildings, 2016. **128**: p. 617-638.
16. Santamouris, M. and K. Vasilakopoulou, *Present and future energy consumption of buildings: Challenges and opportunities towards decarbonisation*. e-Prime-Advances in Electrical Engineering, Electronics and Energy, 2021. **1**: p. 100002.
17. Mandal, J., et al., *Paints as a scalable and effective radiative cooling technology for buildings*. Joule, 2020. **4**(7): p. 1350-1356.
18. Feng, J., et al., *The heat mitigation potential and climatic impact of super-cool broadband radiative coolers on a city scale*. Cell Reports Physical Science, 2021. **2**(7).
19. Santamouris, M. and G.Y. Yun, *Recent development and research priorities on cool and super cool materials to mitigate urban heat island*. Renewable Energy, 2020. **161**: p. 792-807.
20. Santamouris, M., et al., *Progress in urban greenery mitigation science–assessment methodologies advanced technologies and impact on cities*. Journal of Civil Engineering and Management, 2018. **24**(8): p. 638-671.
21. Feng, J., et al., *Overheating of Cities - Magnitude, Characteristics, Impact, Mitigation and Adaptation and Future Challenges*. Annual Review of Environment and Resources, 2023. **In Press**.
22. Hong, T., et al., *Ten questions on urban building energy modeling*. Building and Environment, 2020. **168**: p. 106508.
23. Santamouris, M., *Cooling the cities—a review of reflective and green roof mitigation technologies to fight heat island and improve comfort in urban environments*. Solar energy, 2014. **103**: p. 682-703.
24. Adilkhanova, I., M. Santamouris, and G.Y. Yun, *Coupling urban climate modeling and city-scale building energy simulations with the statistical analysis: Climate and energy implications of high albedo materials in Seoul*. Energy and Buildings, 2023. **290**: p. 113092.
25. Garshasbi, S., et al., *On the energy impact of cool roofs in Australia*. 2023. **278**: p. 112577.
26. Kottek, M., et al., *World map of the Köppen-Geiger climate classification updated*. 2006.
27. Ngarambe, J., M. Santamouris, and G.Y. Yun, *The impact of urban warming on the mortality of vulnerable populations in seoul*. Sustainability, 2022. **14**(20): p. 13452.
28. Oleson, K.W., et al., *Interactions between urbanization, heat stress, and climate change*. Climatic Change, 2015. **129**: p. 525-541.
29. Bhattacharjee, S., et al. *Assessment of different methodologies for mapping urban heat vulnerability for Milan, Italy*. in *IOP conference series: Earth and environmental science*. 2019. IOP Publishing.
30. Santamouris, M., et al., *On the energy impact of urban heat island in Sydney: Climate and energy potential of mitigation technologies*. 2018. **166**: p. 154-164.
31. Khan, A., et al., *Exploring the meteorological impacts of surface and rooftop heat mitigation strategies over a tropical city*. Journal of Geophysical Research: Atmospheres, 2023. **128**(8): p. e2022JD038099.
32. Gao, K. and M. Santamouris, *The use of water irrigation to mitigate ambient overheating in the built environment: Recent progress*. Building and Environment, 2019. **164**: p. 106346.
33. Gao, K., M. Santamouris, and J. Feng, *On the efficiency of using transpiration cooling to mitigate urban heat*. Climate, 2020. **8**(6): p. 69.
34. Vahmani, P. and G.J.G.R.L. Ban-Weiss, *Climatic consequences of adopting drought-tolerant vegetation over Los Angeles as a response to California drought*. 2016. **43**(15): p. 8240-8249.
35. Santamouris, M. and P. Osmond, *Increasing Green Infrastructure in Cities: Impact on Ambient Temperature, Air Quality and Heat-Related Mortality and Morbidity*. Buildings, 2020. **10**(12): p. 233.
36. Santamouris, M., et al., *Passive and active cooling for the outdoor built environment – Analysis and assessment of the cooling potential of mitigation technologies using performance data from 220 large scale projects*. Solar Energy, 2017. **154**: p. 14-33.

37. Ballinas, M. and V.L. Barradas, *The urban tree as a tool to mitigate the urban heat island in Mexico City: A simple phenomenological model*. Journal of environmental quality, 2016. **45**(1): p. 157-166.
38. Broadbent, A.M., et al., *The cooling effect of irrigation on urban microclimate during heatwave conditions*. Urban climate, 2018. **23**: p. 309-329.
39. Lobell, D.B., et al., *Irrigation cooling effect on temperature and heat index extremes*. Geophysical Research Letters, 2008. **35**(9).
40. Coutts, A.M., et al., *Assessing practical measures to reduce urban heat: Green and cool roofs*. Building and Environment, 2013. **70**: p. 266-276.
41. Duarte, D.H.S., et al., *The impact of vegetation on urban microclimate to counterbalance built density in a subtropical changing climate*. Urban Climate, 2015. **14**: p. 224-239.
42. Nyelele, C., C.N. Kroll, and D.J. Nowak, *Present and future ecosystem services of trees in the Bronx, NY*. Urban Forestry & Urban Greening, 2019. **42**: p. 10-20.
43. Rosenzweig, C., et al., *Mitigating New York City's heat island with urban forestry, living roofs, and light surfaces*. 2006: p. 1-5.
44. Teskey, R., et al., *Responses of tree species to heat waves and extreme heat events*. Plant, Cell & Environment, 2015. **38**(9): p. 1699-1712.
45. Allen, C.D., et al., *A global overview of drought and heat-induced tree mortality reveals emerging climate change risks for forests*. Forest Ecology and Management, 2010. **259**(4): p. 660-684.
46. Reich, P.B., et al., *Boreal and temperate trees show strong acclimation of respiration to warming*. Nature, 2016. **531**(7596): p. 633-636.
47. Forster, M. and A. Englefield, *Can soils assist grapevines in coping with heatwaves?* Soil Science Australia, 2018. **186**.
48. Ameye, M., et al., *The effect of induced heat waves on Pinus taeda and Quercus rubra seedlings in ambient and elevated CO₂ atmospheres*. New Phytologist, 2012. **196**(2): p. 448-461.
49. Harfouche, A., R. Meilan, and A. Altman, *Tree genetic engineering and applications to sustainable forestry and biomass production*. Trends in Biotechnology, 2011. **29**(1): p. 9-17.
50. Taha, H., *Meteorological, emissions and air-quality modeling of heat-island mitigation: recent findings for California, USA*. International Journal of Low-Carbon Technologies, 2015. **10**(1): p. 3-14.
51. Selmi, W., et al., *Air pollution removal by trees in public green spaces in Strasbourg city, France*. Urban Forestry & Urban Greening, 2016. **17**: p. 192-201.
52. Taha, H., *Cool Cities: Counteracting Potential Climate Change and its Health Impacts*. Current Climate Change Reports, 2015. **1**(3): p. 163-175.
53. Calfapietra, C., et al., *Role of Biogenic Volatile Organic Compounds (BVOC) emitted by urban trees on ozone concentration in cities: A review*. Environmental Pollution, 2013. **183**: p. 71-80.
54. Arghavani, S., H. Malakooti, and A.A. Bidokhti, *Numerical evaluation of urban green space scenarios effects on gaseous air pollutants in Tehran Metropolis based on WRF-Chem model*. Atmospheric Environment, 2019. **214**: p. 116832.
55. Taha, H., *Modeling impacts of increased urban vegetation on ozone air quality in the South Coast Air Basin*. Atmospheric Environment, 1996. **30**(20): p. 3423-3430.
56. Konopacki, S. and H. Akbari, *Energy savings for heat-island reduction strategies in Chicago and Houston (including updates for Baton Rouge, Sacramento, and Salt Lake City)*. 2002: United States.
57. Haddad, S., et al., *Integrated assessment of the extreme climatic conditions, thermal performance, vulnerability, and well-being in low-income housing in the subtropical climate of Australia*. Energy and Buildings, 2022. **272**: p. 112349.
58. Akbari, H. and S. Konopacki, *Energy effects of heat-island reduction strategies in Toronto, Canada*. Energy, 2004. **29**(2): p. 191-210.

59. Silva, H. and B.S. Fillpot, *Modeling nexus of urban heat island mitigation strategies with electricity/power usage and consumer costs: a case study for Phoenix, Arizona, USA*. Theoretical and Applied Climatology, 2018. **131**(1): p. 661-669.
60. Morakinyo, T.E., et al., *Performance of Hong Kong's common trees species for outdoor temperature regulation, thermal comfort and energy saving*. Building and Environment, 2018. **137**: p. 157-170.
61. Castaldo, V.L., et al., *How outdoor microclimate mitigation affects building thermal-energy performance: A new design-stage method for energy saving in residential near-zero energy settlements in Italy*. Renewable Energy, 2018. **127**: p. 920-935.
62. Kikegawa, Y., et al., *Impacts of city-block-scale countermeasures against urban heat-island phenomena upon a building's energy-consumption for air-conditioning*. Applied Energy, 2006. **83**(6): p. 649-668.
63. Kong, F., et al., *Energy saving potential of fragmented green spaces due to their temperature regulating ecosystem services in the summer*. Applied Energy, 2016. **183**: p. 1428-1440.
64. Yenneti, K., et al. *Urban Overheating and Cooling Potential in Australia: An Evidence-Based Review*. Climate, 2020. **8**, DOI: 10.3390/cli8110126.
65. Garshasbi, S., et al., *Urban mitigation and building adaptation to minimize the future cooling energy needs*. Solar Energy, 2020. **204**: p. 708-719.
66. Santamouris, M., *Using cool pavements as a mitigation strategy to fight urban heat island—A review of the actual developments*. Renewable and Sustainable Energy Reviews, 2013. **26**: p. 224-240.
67. Karlessi, T., et al., *Development and testing of PCM doped cool colored coatings to mitigate urban heat island and cool buildings*. Building and Environment, 2011. **46**(3): p. 570-576.
68. Karlessi, T., et al., *Development and testing of thermochromic coatings for buildings and urban structures*. Solar Energy, 2009. **83**(4): p. 538-551.
69. Santamouris, M. and F. Fiorito, *On the impact of modified urban albedo on ambient temperature and heat related mortality*. Solar Energy, 2021. **216**: p. 493-507.
70. Khan, A., et al. *Optically Modulated Passive Broadband Daytime Radiative Cooling Materials Can Cool Cities in Summer and Heat Cities in Winter*. Sustainability, 2022. **14**, DOI: 10.3390/su14031110.
71. Ulpiani, G., et al., *On the energy modulation of daytime radiative coolers: A review on infrared emissivity dynamic switch against overcooling*. Solar Energy, 2020. **209**: p. 278-301.
72. Tang, K., et al., *Temperature-adaptive radiative coating for all-season household thermal regulation*. Science, 2021. **374**(6574): p. 1504-1509.
73. Khan, A., et al., *On the winter overcooling penalty of super cool photonic materials in cities*. Solar Energy Advances, 2021. **1**: p. 100009.
74. Jeon, S., et al., *Multifunctional Daytime Radiative Cooling Devices with Simultaneous Light-Emitting and Radiative Cooling Functional Layers*. ACS Applied Materials & Interfaces, 2020. **12**(49): p. 54763-54772
75. Chen, F. and J. Dudhia, *Coupling an advanced land surface–hydrology model with the Penn State–NCAR MM5 modeling system. Part I: Model implementation and sensitivity*. Monthly weather review, 2001. **129**(4): p. 569-585.
76. Hong, T., et al., *CityBES: A web-based platform to support city-scale building energy efficiency*. Urban Computing, 2016. **14**: p. 2016.
77. Chen, Y., T. Hong, and M.A. Piette, *City-scale building retrofit analysis: a case study using CityBES*. Build. Simul, 2017.
78. Chen, Y., T. Hong, and M.A. Piette, *Automatic generation and simulation of urban building energy models based on city datasets for city-scale building retrofit analysis*. Applied Energy, 2017. **205**: p. 323-335.
79. Paolini, R., et al., *The hygrothermal performance of residential buildings at urban and rural sites: Sensible and latent energy loads and indoor environmental conditions*. Energy and Buildings, 2017. **152**: p. 792-803.

Tables

Table 1. Description of the mitigation scenarios

No.	Mitigation scenario	Description
1	Reference	Reference Riyadh: Climatic evaluation of the whole Riyadh area for 3 summer months and one winter month under the existing conditions without application of mitigation measures (albedo of roofs and pavements: 0.20).
2	Use of high albedo material	Reflective Riyadh: Modified high albedo in the whole city of Riyadh using reflective materials. Roofs and pavements with higher albedo than the base case is considered for the whole urban area of Riyadh (albedo of roofs: 0.75, albedo of pavements: 0.40).
3	Use of supercool material	Very Reflective Riyadh: Modified very high albedo in the whole city of Riyadh. Citywide implementation of super cool materials, (photonic Day Time Radiative Coolers), in roofs with an albedo of 0.95 and emissivity in the atmospheric window of 0.95. No modification of the albedo of pavements, as under the current conditions.
4	30% low-level non-irrigated vegetation cover	Green and Dry Riyadh: Increase of the green infrastructure of Riyadh up to 30% of its surface using non-irrigated low-level vegetation (shrubs and grass). Albedo as under the current conditions.
5	60% low-level non-irrigated vegetation cover	Very Green and Dry Riyadh: Increase of the green infrastructure of Riyadh up to 60% of its surface, using non-irrigated low-level vegetation (shrubs and grass). Albedo as under the current conditions.
6	30% low-level non-irrigated vegetation cover	Green and Irrigated Riyadh: Increase of the green infrastructure of Riyadh up to 30% of its surface, using irrigated low-level vegetation (shrubs and grass). Albedo as under the current conditions.
7	60% high level irrigated vegetation cover	Very Green and Irrigated Riyadh: Increase of the green infrastructure of Riyadh up to 60% of its surface, using irrigated high-level vegetation (broadleaf trees). Albedo as under the current conditions.
8	Combination of 60% low-level non-irrigated vegetation cover and supercool material.	Very Green – Very Reflective and Dry Riyadh: Combined case - increase of the green infrastructure of Riyadh up to 60% of its surface, using non-irrigated low-level vegetation (shrubs and grass) combined with citywide implementation of super cool materials in roofs with an albedo of 0.95 and emissivity of 0.95. No modification of the albedo of pavements, as under the current conditions.
9	Combination of 60% high-level irrigated vegetation cover and supercool material.	Very Green – Very Reflective and Irrigated Riyadh: Combined case - increase of the green infrastructure of Riyadh up to 60% of its surface, using irrigated high-level vegetation (broadleaf trees) combined with citywide implementation of super cool materials in roofs with an albedo of 0.95 and emissivity of 0.95. No modification of the albedo of pavements, as under the current conditions.

Table 2. Simulated Performance of the Eight Mitigation Scenarios during the summer period as compared to the Reference Scenario.

Scenario	Reflective Riyadh	Very Reflective Riyadh	Green and Dry Riyadh	Green and Irrigated Riyadh	Very Green Non- Irrigated Riyadh	Very Green and Irrigated Riyadh	Very Green – Very Reflective and Dry Riyadh	Very Green – Very Reflective and Irrigated Riyadh
Decrease Max Summer Ambient Temperature at 14:00 pm	2.2	2.3	1.3	1.3	0.8	2.1	1.6	3.0
Decrease of the Mean Summer Ambient Temperature at 14:00 pm	1.2	1.3	-0.1	0.3	-0.3	0.6	0.5	1.4
Decrease of the Min Summer Ambient Temperature at 14:00 pm	0.2	0.3	-1.5	-0.7	-1.4	-0.9	-0.6	0.0
Decrease of the Max Summer Ambient Temperature at 06:00 am	3.4	3.7	3.3	3.7	5.1	7.0	7.4	8.6
Decrease of the Mean Summer Ambient Temperature at 06:00 am	1.2	1.4	0.3	1.1	0.9	2.1	2.1	3
Decrease of the Min Summer Ambient Temperature at 6:00 am	1.1	-0.9	-2.8	-1.5	-3.7	-2.8	-3.6	-2.8
Decrease of the Max 24 h Summer Ambient Temperature	1.9	2.0	4.0	2.6	8.0	7.2	8.5	7.5
Decrease of the Mean 24 h Summer Ambient Temperature	0.9	0.9	0.7	1.2	2.3	3.5	2.9	4.2
Decrease of the 24 h Min Summer Ambient Temperature at 6:00 am	-0.6	-0.6	-2.9	0.2	-1.1	0.4	-0.3	1.3
Decrease of the Max Summer Surface Temperature at 14:00 pm	6.2	6.6	1.6	4.6	1.7	4.6	5.0	7.3
Decrease of the Mean Summer Surface Temperature at 14:00 pm	4.8	5.2	-0.4	2.0	-0.8	2.3	2.6	4
Decrease of the Min Summer Surface Temperature at 14:00 pm	3.5	3.7	-2.5	0.1	-3.3	0.1	0.2	3.5

Table 3. Average Summer Cooling Load of all buildings as well as cooling energy conservation percentage under the reference and the eight considered mitigation scenarios

Scenario	Reference Riyadh	Reflective Riyadh	Very Reflective Riyadh	Green and Dry Riyadh	Green and Irrigated Riyadh	Very Green Non- Irrigated Riyadh	Very Green and Irrigated Riyadh	Very Green – Very Reflective and Dry Riyadh	Very Green – Very Reflective and Irrigated Riyadh
Average Summer Cooling Load, (kWh/m ²)	104.6	100.0	99.2	100.5	98.9	93.5	90.6	89.1	87.9
Reduction of the Cooling Load against the Reference, (%)	4.4	5.2	3.9	5.4	10.6	13.4	14.8	16.0

Table 4. Total Reduction of the total summer Cooling Load of the 3323 buildings, (GWh), calculated under the combined energy retrofitting and heat mitigation simulation and the single heat mitigation simulation settings for the eight mitigation scenarios.

Scenario	Reflective Riyadh	Very Reflective Riyadh	Green and Dry Riyadh	Green and Irrigated Riyadh	Very Green Non- Irrigated Riyadh	Very Green and Irrigated Riyadh	Very Green – Very Reflective and Dry Riyadh	Very Green – Very Reflective and Irrigated Riyadh
Combined Cooling Load Reduction, (GWh)	60.0	57.8	55.6	57.8	68.9	71.2	73.4	77.8
Cooling Load Reduction caused by the Heat Mitigation Measures, (GWh)- Non- Combined Simulation	9.8	11.5	8.7	12.1	23.6	29.8	33.0	35.5
Additional Cooling Load Reduction when retrofitting measures are considered, combined simulation, (GWh)	50.3	46.3	46.9	45.7	45.3	41.4	40.4	42.3
Potential Percentage Contribution of the Heat Mitigation Measures (%)	16	20	16	21	34	42	45	46

Figures

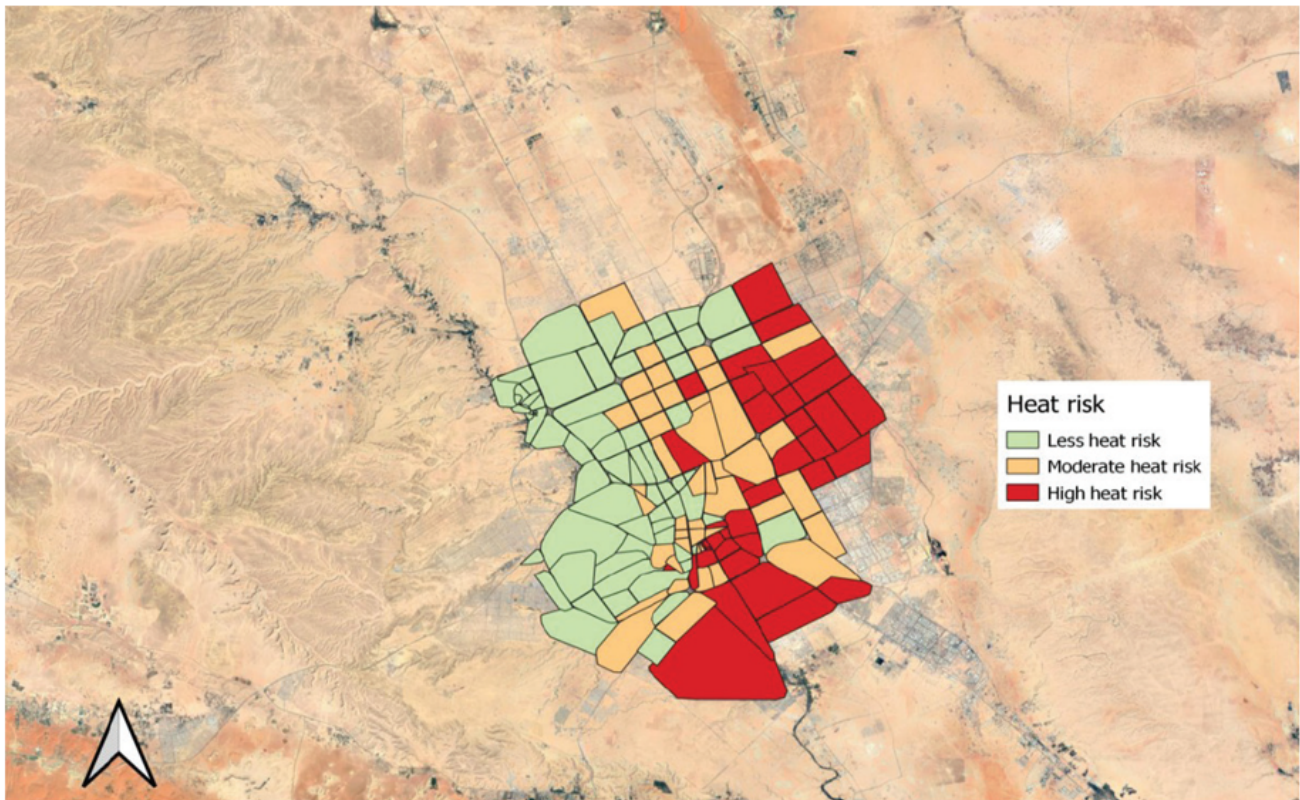


Figure 1

Composite heat indicator of Riyadh.



Figure 2

Distribution of the calculated annual cooling load of the buildings under the reference conditions.

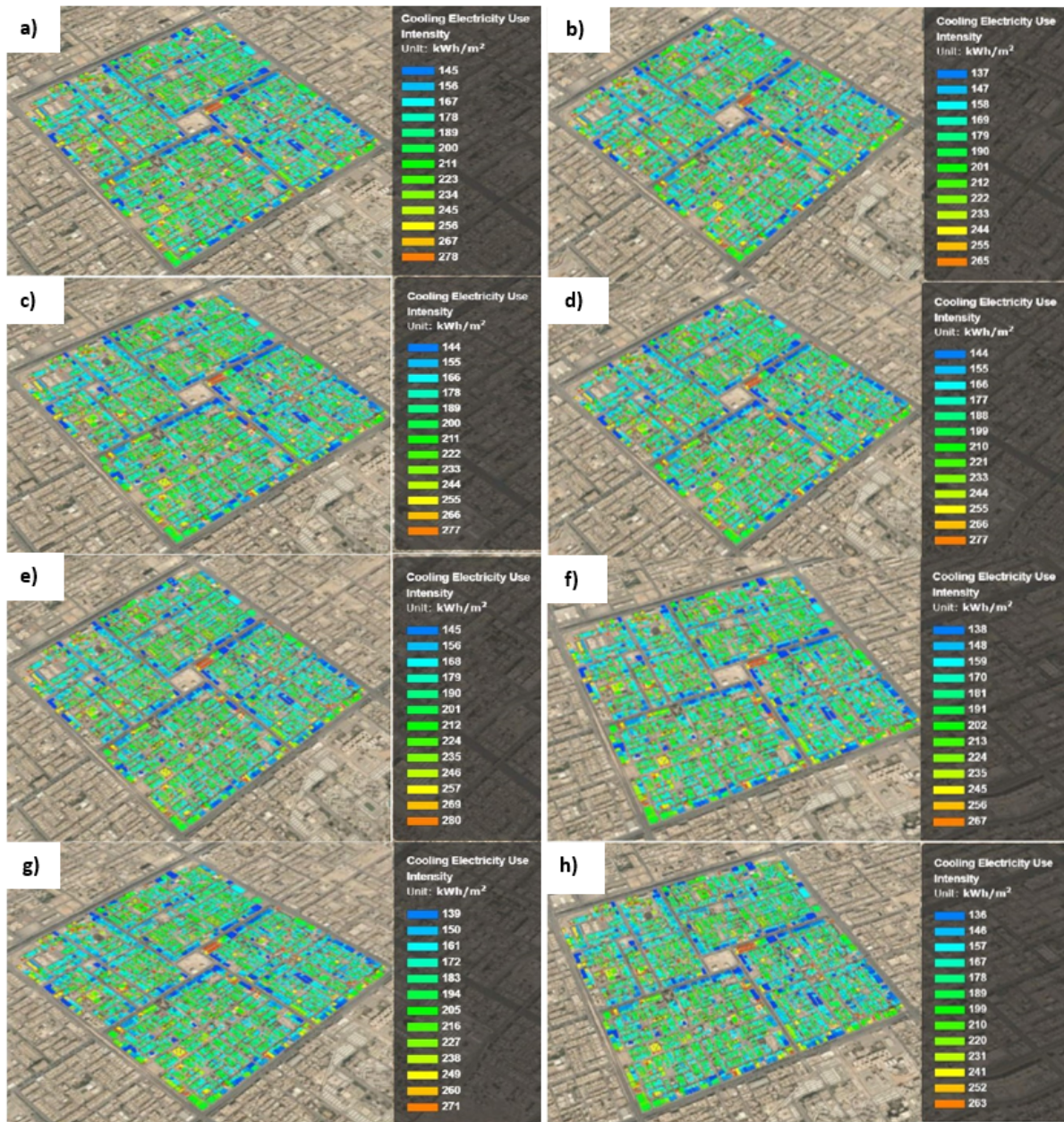


Figure 3

The distribution of the annual cooling load of the buildings for the eight mitigation scenarios: a) Reflective Riyadh, b) Very Reflective and Dry Riyadh, c) Very Reflective Riyadh, d) Green and Irrigated Riyadh, e) Green and Dry Riyadh, f) Very Green and Irrigated Riyadh, g) Very Green and Dry Riyadh, h) Very Reflective and Irrigated Riyadh.

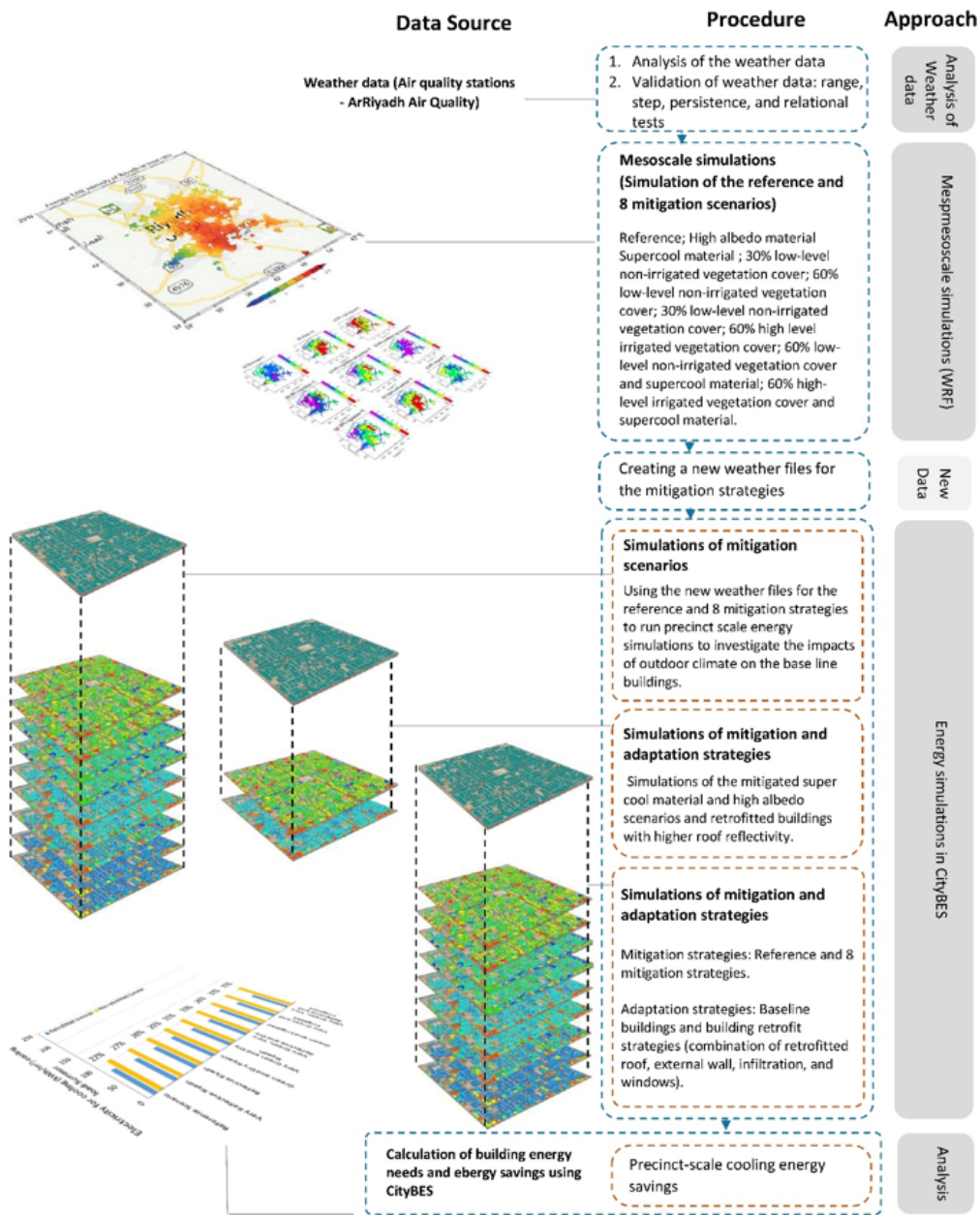


Figure 4

Main methodological approaches and framework used in this study.

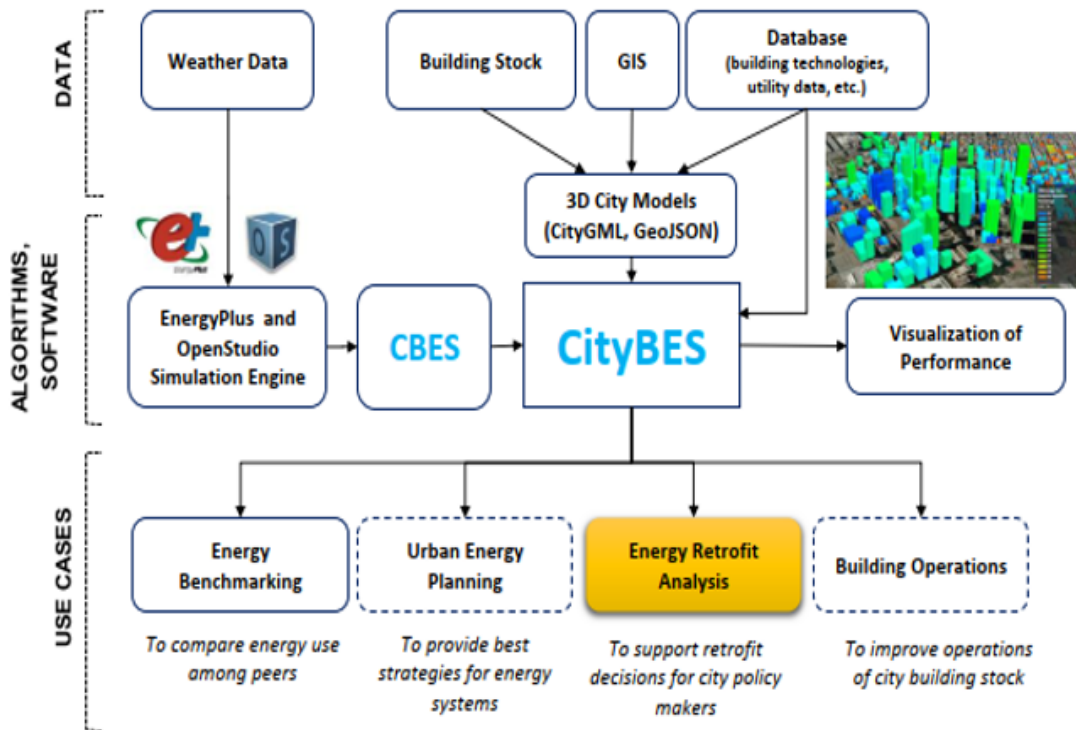


Figure 5

CityBES key components, data flow, and use cases. Image obtained from [28].

Supplementary Files

This is a list of supplementary files associated with this preprint. Click to download.

- [Supplement1MSSH02.docx](#)
- [supplement2MSSH02.docx](#)